Cell

# Deficiency of FANCD2-Associated Nuclease KIAA1018/FAN1 Sensitizes Cells to Interstrand Crosslinking Agents

Katja Kratz,[1,4] Barbara Schöpf,[1,4] Svenja Kaden,[1,4] Ataman Sendoel,[2] Ralf Eberhard,[2] Claudio Lademann,[1] Elda Cannavó,[1,5] Alessandro A. Sartori,[1] Michael O. Hengartner,[2] and Josef Jiricny[1,3,*]

[1]Institute of Molecular Cancer Research, University of Zurich
[2]Institute of Molecular Life Sciences, University of Zurich
[3]Department of Biology
ETH Zurich, Winterthurerstrasse 190, 8057 Zurich, Switzerland
[4]These authors contributed equally to this work
[5]Present address: Department of Microbiology, University of California, Davis, CA 95616-8665, USA
*Correspondence: jiricny@imcr.uzh.ch
DOI 10.1016/j.cell.2010.06.022

## SUMMARY

Cytotoxicity of cisplatin and mitomycin C (MMC) is ascribed largely to their ability to generate interstrand crosslinks (ICLs) in DNA, which block the progression of replication forks. The processing of ICLs requires the *Fanconi anemia* (FA) pathway, excision repair, and translesion DNA synthesis (TLS). It also requires homologous recombination (HR), which repairs double-strand breaks (DSBs) generated by cleavage of the blocked replication forks. Here we describe KIAA1018, an evolutionarily conserved protein that has an N-terminal ubiquitin-binding zinc finger (UBZ) and a C-terminal nuclease domain. KIAA1018 is a 5′→3′ exonuclease and a structure-specific endonuclease that preferentially incises 5′ flaps. Like cells from FA patients, human cells depleted of KIAA1018 are sensitized to ICL-inducing agents and display chromosomal instability. The link of KIAA1018 to the FA pathway is further strengthened by its recruitment to DNA damage through interaction of its UBZ domain with monoubiquitylated FANCD2. We therefore propose to name KIAA1018 FANCD2-associated nuclease, FAN1.

## INTRODUCTION

The *Fanconi anemia* (FA) pathway (Figure 1A) plays a key role in interstrand crosslink (ICL) metabolism in higher eukaryotes by coordinating S phase arrest and DNA repair (Moldovan and D'Andrea, 2009; Thompson and Hinz, 2009). Replication fork blockage activates the ataxia telangiectasia and RAD3-related (ATR) kinase (Pichierri and Rosselli, 2004), which phosphorylates members of the FA core complex (Meetei et al., 2003) composed of FANCA, B, C, E, F, G, L, and FAAP100. The activated complex then associates with FANCM-FAAP24, a DNA translocase (Gari et al., 2008), which activates the E3 ligase FANCL that subsequently ubiquitylates FANCD2-FANCI (Thompson and Hinz, 2009). The latter posttranslational modifications license the processing of the blocked replication fork (Figure 1A), which involves pausing of the fork, incision, lesion unhooking, translesion DNA synthesis (TLS), and homologous recombination (HR) (Moldovan and D'Andrea, 2009). FANCJ, a 5′→3′ DNA helicase, appears to be involved in the late stages of ICL repair (Bridge et al., 2005). Its action would give rise to 3′ flaps, preferred substrates of both endonucleases implicated in ICL processing to date, MUS81/EME1 and XPF/ERCC1.

Recently, several laboratories found interaction between FA proteins and polypeptides involved in mismatch repair (Peng et al., 2007; Zhang et al., 2002). Our analysis of the MLH1 interactome (Cannavo et al., 2007) identified FANCJ among the strongest interactors. Another strong MLH1 interactor was KIAA1018, a hypothetical protein predicted (Kinch et al., 2005; Kosinski et al., 2005) to contain a RAD18-like ubiquitin-binding zinc finger near its N terminus and a C-terminal endonuclease domain. Given the importance of ubiquitylation in the FA pathway (Moldovan and D'Andrea, 2009), and the fact that the putative endonuclease domain of KIAA1018 belongs to the same enzyme superfamily as those present in MUS81 and XPF, we asked whether KIAA1018 is related to FA and how mismatch repair (MMR) might be linked to this branch of DNA repair. Hence, we decided to characterize KIAA1018 and to study its role in DNA metabolism. We now show that KIAA1018 is a nuclease involved in the processing of mitomycin C (MMC)- and cisplatin-induced DNA damage, to which it is recruited by ubiquitylated FANCD2.

## RESULTS

### KIAA1018 Contains Evolutionarily Conserved Zinc Finger and Endonuclease Domains

Analysis of MLH1 and PMS2 interactomes (Cannavo et al., 2007) identified several peptides originating from the human *KIAA1018* open reading frame (ORF), which encodes a polypeptide of 1017

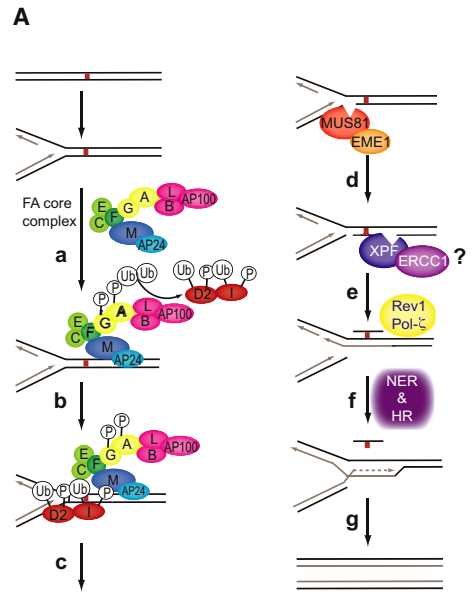


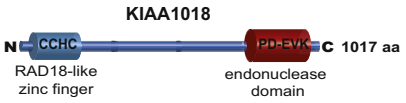


C

```
hsap   29 SIISCFNNAPPAKLACPVCSKMVPRYDLNRHLDEMCA 65
mmus   29 SITSYFNSAPPAKLACSTCHKMVPRYDLIRHLDESCA 65
ggal   45 SIISFFNNVPPAKVTCPVCGQMVPRYGINQHMDELCQ 81
cele   24 SIMAAFEKQSRGKI-CPLCETKFSLASYKSHMN-TCN 58
```

D

```
hsap    958 LPDLVVWNSQSRHFKLVEVKGPND 981
mmus    961 LPDLVVWNSQSHHCKLVEVKGPSD 984
ggal    975 LPDLVVWSTHSNHFKLVEVKGPND 998
cele    808 FPDLTLWNPETKRVAVVEVKGPGD 831
```

E

```
hsKIAA1018    LPDLVVWNSQSRHFKLVEVKGPND
hsXPF         VGDYILTP-----EMCVERKSISD
scRad1        VGDYVITP-----DICLERKSISD
hsMUS81       VGDFVWVA-X16-DHIVERKRLDD
scMUS81       LGDIIWVA-X11-NTIVERKRLDD
```

**Figure 1. Schematic Representation of the FA Pathway and Evolutionary Conservation of KIAA1018**

(A) A consensus model of interstrand crosslink repair (Moldovan and D'Andrea, 2009; Wang, 2007). Upon stalling of the replication fork, the FA core complex is phosphorylated on several subunits by ATR and recruited to the lesion by FANCM/FAAP24. This interaction activates the E3 ligase activity of FANCL (a), which monoubiquitylates the FANCD2/FANCI heterodimer (b). The fork is then cleaved by MUS81 on one side and unhooked by XPF/ERCC1 on the other (c and d). Translesion polymerases then fill the gap opposite the unhooked oligonucleotide (e), which is released by excision repair (f). The collapsed replication fork is then rescued by the HR machinery, including FANCD1 (BRCA2), FANCN (PALB2), and likely also FANCJ (f and g).

amino acids (aa). Its N-terminal region was predicted to contain a RAD18-like CCHC zinc finger, a so-called UBZ domain, present in proteins that bind ubiquitylated polypeptides (Hofmann, 2009). The C-terminal portion of KIAA1018 was suggested to contain an endonuclease domain of the PD-D/E(X)K type (Kinch et al., 2005; Kosinski et al., 2005) (Figure 1B).

Alignment of the aa sequences of human, murine, avian, and *C. elegans* KIAA1018 revealed a high degree of evolutionary conservation, particularly in the UBZ region (Figure 1C) and in the putative endonuclease PD-D/E(X)K motif (Figure 1D), which is found in other DNA repair proteins, such as the bacterial MMR protein MutH, certain restriction enzymes, and, most notably, the eukaryotic MUS81 and XPF/RAD1 endonucleases (Figure 1E).

## Depletion of KIAA1018 Sensitizes Human Cells to Interstrand Crosslinking Agents

We asked whether KIAA1018 deficiency sensitizes cells to a particular type of DNA damage. To this end, we knocked down *KIAA1018* mRNA in HEK293 cells by siRNA targeting exon 3 (Figure 2A) and subjected these cells to treatment with several DNA-damaging agents. Compared to wild-type (WT) controls, the KIAA1018 knockdown cells were not significantly sensitized to X-rays (Figure 2B), UV irradiation (Figure 2C), or camptothecin (Figure 2D). In contrast, KIAA1018-deficient cells were hypersensitive to the ICL-inducing agents MMC (Figure 2E) and cisplatin (Figure 2F), similarly to cells deficient in FANCJ (Figures 2A, 2E, and 2F). siRNA targeting exon 5 yielded similar results (data not shown); the above phenotype was thus not caused by an off-site effect of the siRNA.

## KIAA1018 Requires Its Putative Nuclease Domain for Activity

We generated HEK293 cell lines stably expressing KIAA1018 N-terminally fused to the green fluorescent protein (GFP). The *GFP-KIAA1018* fusion cDNAs encoded either the WT enzyme or a variant carrying a D960A (DA) mutation in its predicted nuclease active site. The cDNAs also contained silent mutations in the *KIAA1018* ORF, which made the respective mRNAs resistant to knockdown by exon 3 siRNA. As shown in Figure S1A (available online), the selected clones expressed similar levels of the GFP-WT and GFP-DA variants. Treatment of these cells with Luc siRNA did not affect their sensitivity to MMC. When KIAA1018 siRNA was used, the sensitivity of the GFP-WT clone was also unaffected, whereas the GFP-DA clones were sensitized to MMC treatment (Figure 2G). This result confirms that the phenotype induced by the KIAA1018 siRNA was not due to an off-target effect, demonstrates that the GFP-WT fusion

(B) KIAA1018 is a polypeptide of 1017 aa, containing a predicted N-terminal RAD18-like CCHC zinc finger and a C-terminal endonuclease domain.
Alignments of the zinc finger (C) and endonuclease (D) domains of KIAA1018 from man, mouse, chicken, and worm are shown.
(E) Alignment of the endonuclease domain of human KIAA1018 with those of human MUS81 and XPF and their yeast orthologs Mus81 and Rad1, respectively. Identical residues are shown in bold. The key residues of the zinc finger and endonuclease motifs are boxed. The numbers indicate aa residues flanking these motifs in the respective *KIAA1018* open reading frames. Asterisks mark aa mutated to alanine (see Results).

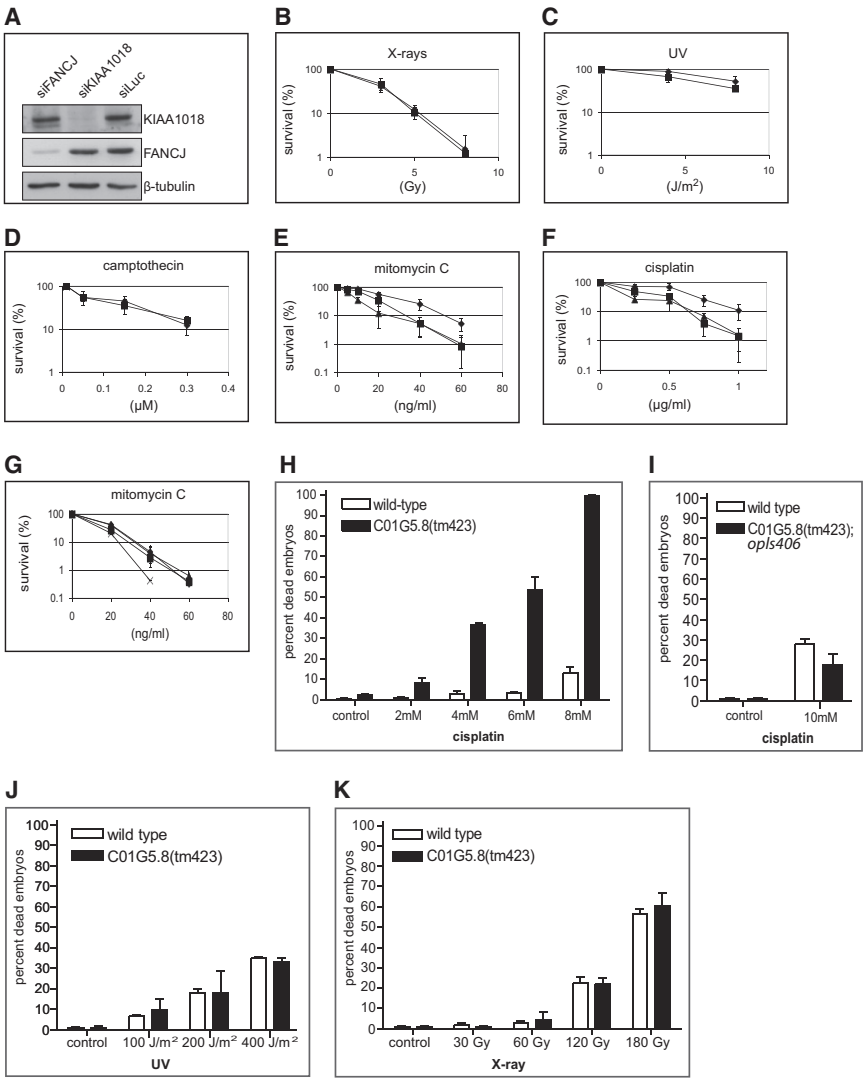


**Figure 2. siRNA Knockdown of KIAA1018 Sensitizes Cells to MMC and Cisplatin**

(A) Western blot showing efficacy of treatment with the indicated siRNAs. Samples were collected 40 hr after siRNA transfection. siLuc served as negative control and β-tubulin as loading control.

(B–F) Clonogenic survival assays of HEK293 cells treated 40 hr after siRNA-mediated KIAA1018 or FANCJ knockdown. KIAA1018-depleted cells and mock-depleted controls were similarly sensitive to X-rays (B), UV radiation (C), and camptothecin (D). siRNA-mediated knockdown of KIAA1018 or FANCJ sensitized cells to MMC (E) and cisplatin (F). Key: (◆) siLuc; (■) siKIAA1018; (▲) siFANCJ.

(G) Clonogenic survival assay with HEK293 cells stably expressing siRNA-resistant GFP-KIAA1018. Cells expressing WT GFP-KIAA1018 showed similar sensitivity to MMC, irrespective of depletion of endogenous KIAA1018. In contrast, expression of GFP-KIAA1018 D960A resulted in increased sensitivity to MMC after depletion of endogenous KIAA1018. Key: (◆) GFP-KIAA1018 WT + siLuc; (■) GFP-KIAA1018 WT + siKIAA1018; (▲) GFP-KIAA1018 D960A + siLuc; (**X**) GFP-KIAA1018 D960A + siKIAA1018. Graphs represent the results of three independent experiments, each carried out in triplicate. Each data point represents an average ± standard deviation (SD).

(H) Increased embryonic lethality of *C01G5.8 (tm423)* mutant animals in response to cisplatin treatment. (I) Rescue of *C01G5.8(tm423)* mutant phenotype by C01G5.8::gfp expression. (J and K) Embryonic lethality after treatment with UV or IR. Synchronized L4 or *opIs406($P_{C01G5.8}$::C01G5.8::gfp::let-858(3′UTR))* animals were exposed to cisplatin for 24 hr (H and I) and were subsequently allowed to lay eggs for 8 hr. For IR and UV treatments (J and K), synchronized young adult animals were allowed to lay eggs for 6–8 hr 24 hr post-treatment. Embryonic lethality was quantified 24 hr later. Data shown represent the average percent embryonic lethality of 20 adult animals ± SD.

See also Figure S1.

protein is functional, and, most importantly, shows that the nuclease domain is indispensable for KIAA1018 function.

## Disruption of the *KIAA1018* Ortholog *C01G5.8* in *C. elegans* Leads to Cisplatin-Induced Embryonic Lethality

KIAA1018 is highly conserved in evolution (Figures 1C and 1D). In order to ascertain that the above-described sensitivity to ICL-inducing agents was not limited to KIAA1018-depleted human cells, we examined the phenotype of *C. elegans* disrupted in the *KIAA1018* ortholog *C01G5.8* (Figure S1B). The *C01G5.8(tm423)* mutant developed similarly to WT (data not shown), which showed that C01G5.8 is not required for normal growth. Cisplatin treatment caused a dramatic increase in embryonic lethality in the *C01G5.8(tm423)* mutants, whereas the viability of WT worms was only slightly impaired (Figure 2H).

We next generated the transgenic *C. elegans* line *opIs406 ($P_{C01G5.8}$::C01G5.8::gfp)* (Figure S1C). Like the human ortholog, the nematode GFP fusion protein overexpressed in this line was functional, as it rescued the cisplatin-sensitive phenotype of the *C01G5.8(tm423)* mutants (Figure 2I). Because treatment with ultraviolet (UV) (Figure 2J) or ionizing radiation (IR) (Figure 2K) had a similar effect on both WT and mutant animals, we conclude that C01G5.8 functions in the repair of cisplatin-induced damage during embryonic development. The sensitization to cisplatin of both human cells and *C. elegans* lacking KIAA1018 or its ortholog C01G5.8 suggests that the function of this protein family in the processing of DNA damage is evolutionarily conserved.

## KIAA1018/C01G5.8 Localization to Subnuclear Foci Is Enhanced by DNA Damage

As the GFP fusion proteins were functional, we decided to study their localization. In actively proliferating cells, namely embryos (Figures 3A and 3B) and germ cells of the mitotic region (Figures 3C and 3D), we observed both an evenly distributed as well as

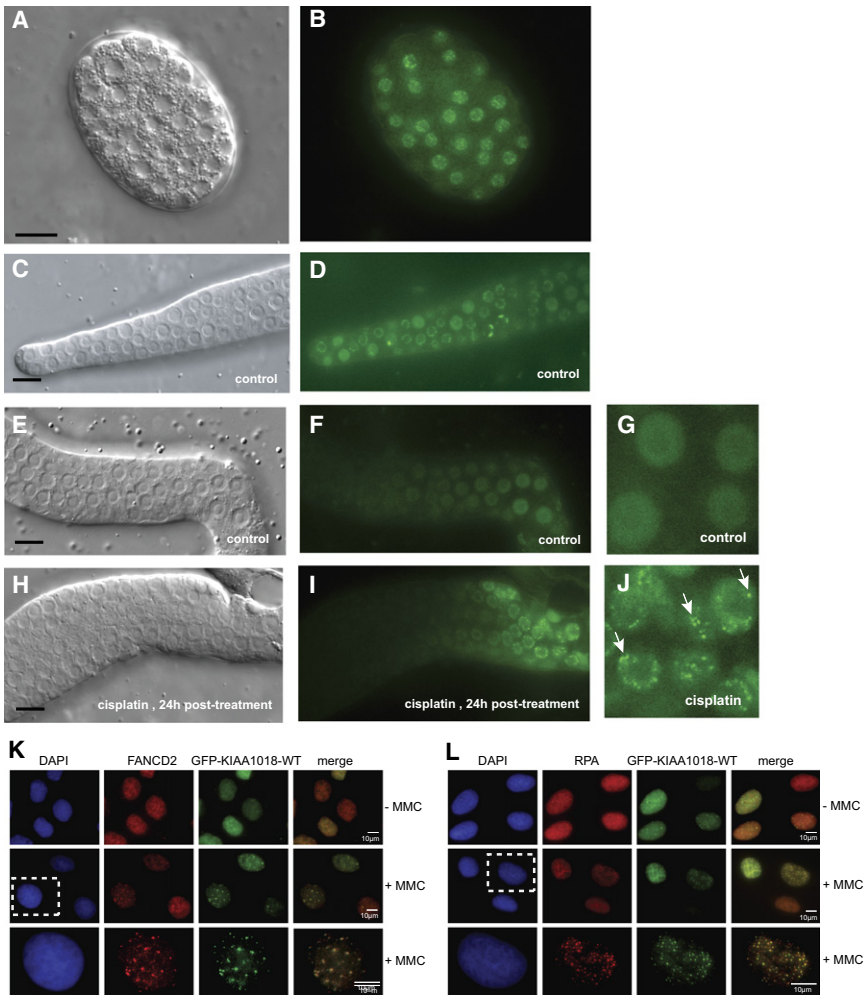


**Figure 3. KIAA1018 Is Recruited to Sites of DNA Damage in *C. elegans* and Human Cells**

(A) C01G5.8 is a nuclear protein expressed in embryos and in the germline of *C. elegans*. C01G5.8::gfp was detected in the nucleus of embryos (A and B), mitotic germline zone (C and D), and late pachytene stage germ cells (E–J) of the transgenic *opIs406[$P_{C01G5.8}$::C01G5.8::gfp::let-858(3′UTR)]* line. Cisplatin treatment resulted in relocalization of C01G5.8::gfp to distinct foci (arrows) (H–J). Scale bars, 10 μm.

Human GFP-KIAA1018-WT colocalizes with FANCD2 (K) and RPA (L) to MMC-induced foci. U2OS cells stably expressing GFP-KIAA1018-WT were mock-treated or treated with MMC (120 ng/ml). After 20 hr, cells were stained with antibodies against FANCD2 (TexasRed) (K) or RPA (TexasRed) (L).

fociform C01G5.8::gfp pattern. In contrast, in pachytene zone germ cells, which are arrested in prophase of meiosis I, C01G5.8::gfp was evenly distributed (Figures 3E–3G) but formed foci upon cisplatin treatment (Figures 3H–3J).

Aggregation in subnuclear foci is a hallmark of proteins participating in DNA-damage response. As C01G5.8::gfp formed foci in cisplatin-treated cells, we wanted to know whether human KIAA1018 acted similarly. Untreated cells contained a small number of foci of GFP-KIAA1018, FANCD2, and Replication Protein A (RPA, marker of long stretches of single-stranded DNA). Upon cisplatin (data not shown) and MMC treatment, the number of foci rose dramatically, and GFP-KIAA1018 colocalized in them with both FANCD2 (Figure 3K) and RPA (Figure 3L).

## FANC Complex Signaling Is Unaffected in KIAA1018-Depleted Cells

Given that sensitivity to ICL-inducing agents is a hallmark of FA cells, and that KIAA1018 colocalizes to DNA-damage foci with FANCD2, we suspected that KIAA1018 might be linked to the FA pathway. We therefore asked whether KIAA1018 deficiency affects activation of the FA complex, which can be detected as monoubiquitylation of FANCD2 and FANCI (Garcia-Higuera et al., 2001; Smogorzewska et al., 2007). As shown in Figure 4A, treatment of HEK293 cells with MMC or hydroxyurea (HU) resulted in substantial FANCD2 ubiquitylation, but this process was unaffected by KIAA1018 knockdown. A similar phenomenon was observed in cells lacking FANCJ (Bridge et al., 2005). Thus, if KIAA1018 were linked to the FA pathway, it would—like FANCJ—act downstream of the FA complex.

## Human Cells Lacking FANCD2, KIAA1018, or Both Proteins Display Similar Sensitivities to MMC

Given that GFP-KIAA1018 and FANCD2 colocalize to DNA-damage-induced foci, we asked whether KIAA1018 and FANCD2 were epistatic. We therefore knocked down KIAA1018 and FANCD2, either singly or together, in HEK293 cells (Figure 4B). As shown in Figure 4C, cells lacking both proteins were not appreciably more sensitive to MMC than cells lacking only one of these polypeptides. This suggests that KIAA1018 might be epistatic with the FA proteins, although a stable system is necessary to exclude the possibility of an incomplete knockdown in cells treated with both siRNAs.

## The Zinc Finger of KIAA1018 Is Necessary and Sufficient for Targeting the Protein to Sites of DNA Damage

KIAA1018 possesses a UBZ motif close to its N terminus (Figures 1B and 1C). In other polypeptides, this motif has been shown to interact with ubiquitylated polypeptides (Hofmann, 2009). In order to characterize the function of the UBZ of KIAA1018, we expressed in *E. coli* glutathione S-transferase (GST) fused to KIAA1018 aa 1–124 containing either the WT UBZ or a variant in which the UBZ was disrupted by mutating cysteines 44 and 47 to alanines (Figure 1C). As zinc finger domains are also known to bind DNA, we tested these peptides in a mobility shift assay, using a homoduplex 38-mer oligonucleotide. We found no

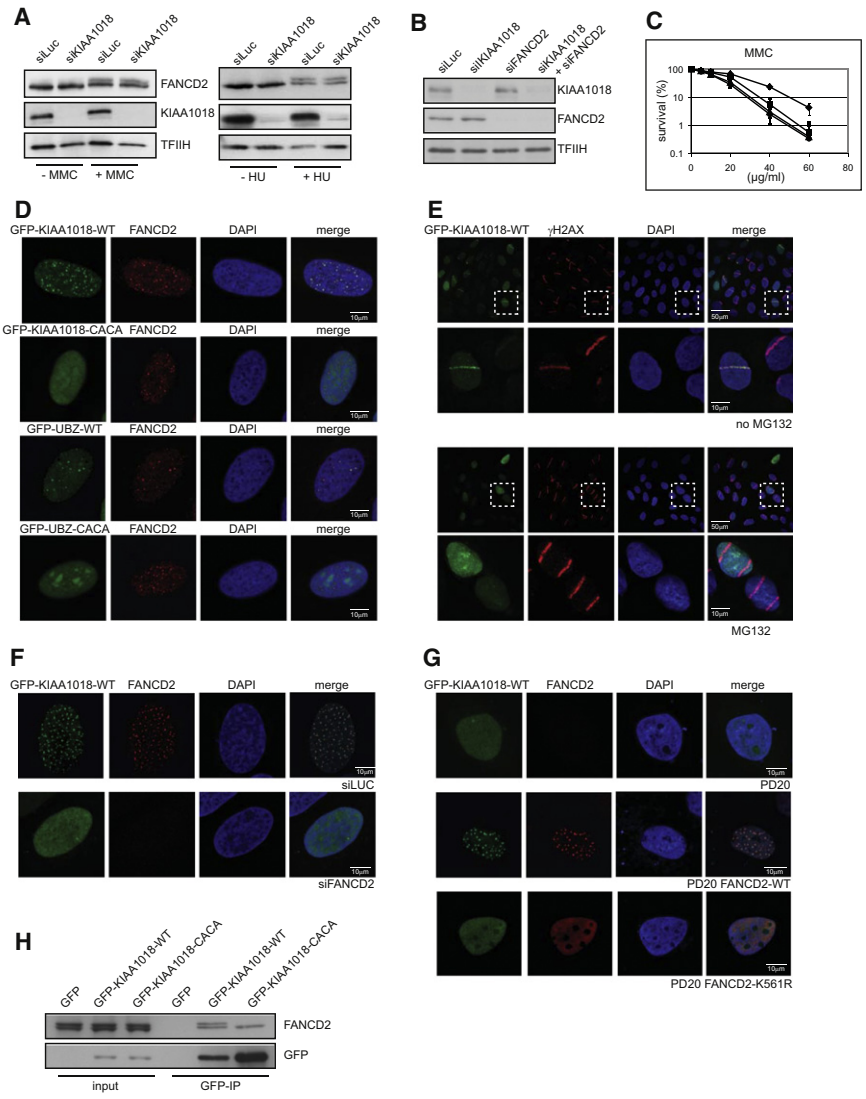


**Figure 4. KIAA1018 Localization to MMC-Induced Foci Requires Ubiquitylation and FANCD2**

(A) Western blot of extracts of HEK293 cells treated or mock-treated with MMC (20 hr) or HU (16 hr) 40 hr after transfection with the indicated siRNAs. The treatments resulted in substantial monoubiquitylation of FANCD2 in both experiments, which shows that KIAA1018 acts downstream (or independently) of the FA complex. TFIIH served as loading control.

(B) Western blot showing KIAA1018 and FANCD2 levels in HEK293 cells 40 hr after treatment with the respective siRNAs. siLuc served as negative control and TFIIH as loading control.

(C) siRNA-mediated knockdown of KIAA1018 or FANCD2 sensitized cells to MMC to a similar extent as a knockdown of both proteins. The results of three independent experiments are shown, each carried out in triplicate. Each data point represents an average ± SD. Key: (◆) siLuc; (■) siKIAA1018; (▲) siFAND2; (●) siKIAA1018 + siFANCD2.

(D) U2OS cells stably expressing GFP-tagged full-length KIAA1018-WT (top row), full-length zinc finger CACA variant (second row), the N-terminal 124 amino acids of WT KIAA1018 containing the zinc finger (third row), or the corresponding CACA zinc finger fragment (bottom row) were treated with 120 ng/ml MMC for 16 hr before immunostaining with FANCD2 antibody. GFP foci are only detectable in cells transfected with vectors expressing KIAA1018 variants with an intact UBZ domain.

(E) U2OS cells stably expressing GFP-KIAA1018-WT were laser microirradiated and immunostained 2 hr later with an antibody against γ-H2AX. Where indicated, cells were incubated with 20 mM MG132 for 120 min before irradiation. GFP-KIAA1018 fails to be recruited to damage stripes in the absence of ubiquitylation.

(F) U2OS cells stably expressing GFP-KIAA1018-WT were treated with luciferase or FANCD2 siRNAs for 48 hr. Treatment with 120 ng/ml MMC for 16 hr was followed by immunostaining with anti-FANCD2 antibody. GFP-KIAA1018 is not recruited to damage foci in the absence of FANCD2.

(G) PD20 (FA-D2) fibroblasts (top row), PD20 fibroblasts stably expressing FANCD2-WT (middle row), or FANCD2-K561R mutant (bottom row) were transiently transfected with GFP-KIAA1018-WT, treated with 120 ng/ml MMC for 16 hr, and immunostained with anti-FANCD2 antibody. GFP-KIAA1018 only localizes to damage foci in cells expressing the WT FANCD2 protein.

(H) Extracts of HEK293 cells stably expressing GFP-KIAA1018-WT or GFP-KIAA1018-CACA and treated with 120 ng/ml MMC were incubated with anti-GFP antibody and the immunoprecipitate was analyzed with antibodies against GFP or FANCD2. GFP-KIAA1018 interacts preferentially with the monoubiqyitylated form of FANCD2.

See Figure S2 for quantifications.

evidence of the GST-fusions interacting with DNA in this assay, even though the mismatch binding factor MutSα bound to the homoduplex (a poor substrate for this protein) under identical conditions (Figure S2A).

We then studied the MMC response of the GFP-KIAA1018 WT and CACA variants stably expressed in U2OS cells. We generated two additional cell lines expressing solely the N-terminal 124 aa residues encoding either the WT or the mutant UBZ. Expression of these variants in U2OS cells, followed by treatment with MMC, resulted in the formation of foci in cells expressing WT GFP-KIAA1018 and the 124 aa UBZ only. These foci colocalized with those formed by FANCD2. In contrast, both KIAA1018-CACA variants diffused throughout the nucleus and failed to form foci upon MMC treatment, even though FANCD2 foci formed normally (Figure 4D and Figure S2B). siRNA-mediated knockdown of endogenous KIAA1018 in cells expressing the KIAA1018 GFP-UBZ fragment did not alter the targeting to the MMC-induced foci, thus excluding the possibility that GFP-UBZ localizes to the damage sites via association with the endogenous protein (data not shown). This

suggested that the UBZ is necessary and sufficient to target GFP-KIAA1018 to DNA-damage foci generated by MMC treatment.

### Recruitment of KIAA1018 to DNA-Damage Foci Is Dependent on FANCD2 Ubiquitylation

We wanted to know whether KIAA1018 targeting to MMC-induced foci was dependent on ubiquitylation, similarly to that described for FANCD2 (Garcia-Higuera et al., 2001). To this end, we pretreated the U2OS cells stably expressing GFP-KIAA1018 with MG132, an inhibitor of the 26S proteasome, which also causes sequestration of ubiquitin in the cytoplasm (Dantuma et al., 2006). We then generated DNA damage by a UV microlaser, which induces a variety of DNA lesions concentrated in micron-thin stripes and causes a substantial perturbation of chromatin structure, which brings about rapid recruitment of the phosphorylated form of the histone variant γ-H2AX. As shown in Figure 4E and Figure S2C, GFP-KIAA1018 and γ-H2AX colocalized in the laser stripes, but the KIAA1018 signal remained diffuse in MG132 pretreated cells. This indicated that KIAA1018 recruitment to DNA damage in chromatin required nuclear ubiquitin.

In the above experiments, we showed that MMC treatment of U2OS cells stably expressing GFP-KIAA1018 induced the formation of KIAA1018 foci (Figures 3K and 3L), that FANCD2 colocalized with GFP-KIAA1018 to these foci (Figure 3K), and that KIAA1018 was recruited to laser-induced stripes in a ubiquitin-dependent manner (Figure 4E). As no KIAA1018 foci were formed in cells in which *FANCD2* mRNA was knocked down with either one of two different siRNAs (Figures 4B and 4F, Figure S2D, and data not shown), we concluded that KIAA1018 recruitment to DNA-damage foci required ubiquitin and FANCD2.

This hypothesis could be further substantiated in the *FANCD2*-mutated cell line PD20, which displayed no MMC-induced foci of GFP-KIAA1018 (Figure 4G, top row; see also Figure S2E). The phenotype of this cell line could be rescued by expression of *FANCD2* cDNA; in the latter cell line, FANCD2 and GFP-KIAA1018 colocalized to MMC-induced foci (Figure 4G, middle row; Figure S2E). In contrast, when the cells were stably transfected with a FANCD2 K561R variant that cannot be ubiquitylated (Garcia-Higuera et al., 2001), both proteins failed to form foci upon MMC treatment (Figure 4G, bottom row; Figure S2E).

The above evidence strongly suggested that KIAA1018 is recruited to MMC-induced foci by monoubiquitylated FANCD2, likely in complex with FANCI. We therefore asked whether KIAA1018 and FANCD2 interact directly. Using anti-GFP antibodies, we immunoprecipitated the GFP-KIAA1018 fusion protein, or its CACA UBZ variant, from extracts of stably transfected, MMC-treated HEK293 cells, and probed the immunoprecipitates for the presence of FANCD2. As shown in Figure 4H, the GFP antibodies pulled down WT GFP-KIAA1018 and both the unmodified and the monoubiquitylated forms of FANCD2. Notably, only the unmodified form was present in the GFP-KIAA1018-CACA pull-down, which shows that KIAA1018 interacts specifically with the monoubiquitylated form of FANCD2 via its UBZ domain.

### KIAA1018 Is a Nuclease

As bioinformatic analysis of the *KIAA1018* ORF predicted the protein to be an endonuclease (Kinch et al., 2005; Kosinski et al., 2005), and given that the protein appears to protect cells against ICL-generating substances, we asked whether the protein is indeed a nuclease.

We expressed full-length KIAA1018 in *E. coli* fused to an N-terminal Nus-His-tag (Ermolova et al., 2003) to aid solubility and purified the fusion protein to apparent homogeneity (Figures S3A and S3B). To test for nucleolytic activity, we deployed a nonspecific endonuclease assay (Kadyrov et al., 2007). Incubation of supercoiled plasmid DNA with increasing amounts of the Nus-His-KIAA1018 fusion protein in the presence of manganese and 100 mM KCl gave rise first to open circular, then linear forms (Figure 5A, Figure S3C), showing that KIAA1018 cleaved the substrate endonucleolytically. At the highest concentrations, the linearized DNA was degraded, which suggested that the enzyme is also an exonuclease. The UBZ-CACA variant was similarly active as the WT enzyme, but the two variants carrying mutations in the putative nuclease active site, D960A (DA) and K977A (KA), were severely impaired at equal protein concentrations (Figure 5A and Figures S3A–S3C). The loss of nuclease activity of the latter two variants was apparently not linked to incorrect folding or other structural perturbation, as the proteins were still able to bind DNA in a gel shift assay (Figure S3D).

Most metal-dependent nucleases can be inhibited either by chelating agents or by zinc or calcium. This is also true for KIAA1018, which could be effectively inhibited by EDTA or by zinc chloride (Figure 5B). The enzyme displayed optimal activity at pH 7.2–7.4 and 25 mM KCl in the presence of manganese. When magnesium was used, the endonucleolytic activity was somewhat reduced, but the degradation of DNA was restricted (Figure S3E). Under optimized conditions and when used in large excess, the KA variant possessed residual nuclease activity in the plasmid relaxation assay (Figure S3F). For this reason, we decided to use the WT and the DA variant in the search for specific substrates of KIAA1018.

### KIAA1018 Preferentially Cleaves 5′ Flaps and Has Both Exo- and Endonuclease Activities

In the above experiments, to aid solubility we used bacterially expressed KIAA1018 carrying a 55 kDa Nus-His tag. In order to ensure that its activity was unaffected by the tag or by the lack of posttranslational modifications, we expressed KIAA1018 and its DA variant in the baculovirus system. An N-terminal maltose-binding protein (MBP) tag was used to express the protein, but this was removed during purification (Figures S4A and S4B). We tested the untagged enzyme on different oligonucleotide structures resembling intermediates of replication and recombination (Figure S4C). We used magnesium as the divalent ion because proteins of the PD-(D/E)XK nuclease superfamily are all magnesium dependent.

We first used substrates labeled at the 5′ end of the top strand (Figure S4C, f9) and could show that KIAA1018 cleaved them in the following order of preference: 5′ flap > > > splayed arm ≈ 3-way junction (3-WJ) > 3′ flap. The principal products were fragments between 31 and 35 nucleotides in length. As the flap was 30 nucleotides long, this indicated that the enzyme cleaved

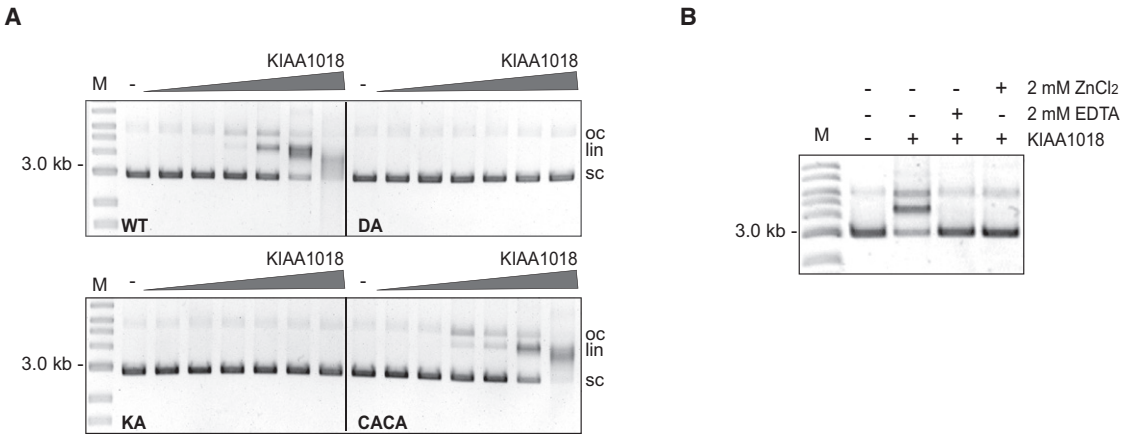


**Figure 5. KIAA1018 Is a Nuclease**

(A) Twenty fmoles of plasmid DNA were incubated with increasing amounts of bacterially expressed Nus-His-KIAA1018. The WT protein and the CACA mutant converted the supercoiled (sc) DNA first to open-circular (oc) and then to linear (lin) forms, whereas the DA and KA mutants did not. The figure is an image of an ethidium bromide-stained 0.8% agarose gel. M: 1 kb marker (NEB), WT: Nus-His-KIAA1018-WT; DA: Nus-His-KIAA1018 mutant D960A; KA: Nus-His-KIAA1018 mutant K977A; CACA: Nus-His-KIAA1018 mutant C44AC47A; (–) no protein.

(B) Inhibition of KIAA1018 endonuclease activity with 2 mM EDTA or 2 mM $ZnCl_2$. M: 1 kb marker, KIAA1018: WT. Assays were carried out in manganese buffer. See Figure S3 for supplemental information.

the substrates in double-stranded (ds) DNA, 1–5 nucleotides downstream from the junction (Figure 6A and Figure S4C, large arrow). In the reactions containing the 3-WJ, 3′ flap, and, to a small extent, also the splayed arm substrate, we also detected very fast-migrating species, which corresponded in length to 2–4 nucleotides. This suggested that KIAA1018 is also a 5′→3′ exonuclease, as already anticipated from the preliminary assays (Figure 5A). We could confirm this by labeling the same substrates at the 5′ end of the bottom strand (Figure 6A). In these assays, all substrates gave rise to a pentamer fragment. (The exonucleolytic cleavage products differed in length between the substrates labeled in the top or the bottom strands because the latter was one nucleotide longer. See Figure S4C.) This shows that KIAA1018 can generate 5′-recessed ends from blunt-ended substrates and that the enzyme makes the first incision ~4 nucleotides into the ds region on these substrates (Figure S4C, small arrows). Interestingly, although the exonuclease activity of KIAA1018 on ds termini was robust, the 5′ flap substrate was processed to yield predominantly the single-stranded (ss) 31- to 35-mer flap and only small amounts of the rapidly migrating species. This suggested that the enzyme did not degrade the cleaved-off ss flap with appreciable efficiency. We could confirm this by incubating the 5′ flap substrate with increasing amounts of enzyme. As shown in Figure 6B, the amount of free ss flap fragments increased with enzyme concentration, but only a minor increase in the high-mobility species was observed.

Next we labeled the substrates at the 3′ end. As shown in Figure 6C, the 5′ flap substrate gave rise to a series of bands ranging in length from approximately 10–29 nucleotides, which represent products of 5′→3′exonucleolytic degradation of the labeled strand after the flap was cleaved off (Figure 6F). Interestingly, while the 5′-labeled 3-WJ (f9 strand) was cleaved with very low efficiency (Figure 6A), the same substrate labeled at the 3′ end of the same (f9) strand appeared to be endonucleolytically cleaved and then exonucleolytically degraded with efficiency similar to the 5′ flap. By 3′-labeling the 30-mer (f7) of the 3-WJ, we could show that this oligomer was rapidly degraded, creating thus a 5′ flap substrate that was then efficiently processed by KIAA1018 (Figure 6D).

The bacterially expressed KIAA1018 used in comparable amounts (Figure S4B) behaved in these assays similarly in magnesium (data not shown) and in manganese (Figures S4D and S4E). However, although manganese increased KIAA1018′s enzymatic activity, it decreased its specificity.

That the cleaved-off 5′ flap (Figures 6A and 6B) was not further processed by the enzyme is supported by the fact that ssDNA was not appreciably bound by the enzyme in a gel shift assay, whereas linear dsDNA, 5′ flap and 3′ flap substrates were bound with similar efficiencies (Figure S4F).

In an attempt to study the substrate preference of KIAA1018 exonuclease, we incubated the enzyme with several different substrates. As shown in Figure 6E and Figure S4G, KIAA1018 exonuclease activity displayed a clear preference for dsDNA substrates containing a recessed 5′ end, a nick, or a gap. Blunt-ended DNA was processed less efficiently and the worst substrates were ssDNA and ss 5′ overhangs, as anticipated from the stability of the cleaved-off 5′ flap (Figure 6B).

To test whether the substrate specificity of KIAA1018 might be altered by an as-yet-unidentified interacting partner, we immunoprecipitated the enzyme from HEK293 cells stably expressing either FLAG-tagged KIAA1018 WT or the DA variant. The immunoprecipitate of the WT enzyme displayed the same substrate preference as the bacterially expressed and the Sf9-expressed proteins (Figures 6A and 6H, Figure S4D). However, it appeared to be more specific, giving rise to a single product upon incubation with the 5′ flap substrate (cf. product in Figure 6A). This change was not due to MLH1, as coexpression of KIAA1018

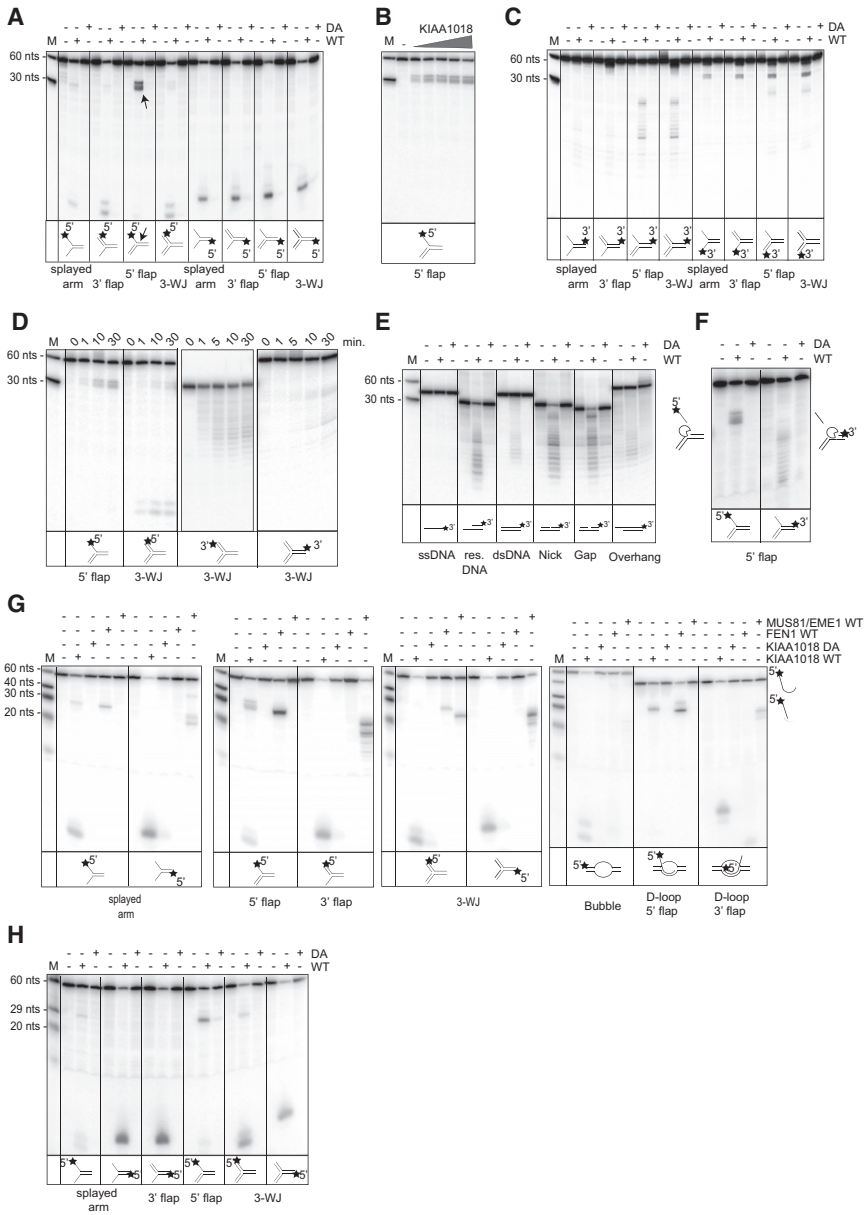


**Figure 6. KIAA1018 Exhibits Preference for 5′ Flaps**

(A) Sf9-expressed KIAA1018-WT and its DA variant were incubated with the indicated substrates (protein to DNA ratio 10:1). KIAA1018 exhibits a preference for 5′ flaps. Asterisk represents $^{32}$P phosphate.

(B) Incubation of WT KIAA1018 (3- to 10-fold excess over DNA) with the 5′ flap substrate for 1 hr at 37°C. The ss product was resistant to KIAA1018 exonuclease.

(C) DNA substrates used in (A) were labeled at the 3′ end (see asterisks) to assess the exonuclease activity of KIAA1018 (10:1 ratio protein to DNA). Following endonucleolytic incision at the flap, KIAA1018 degraded the remaining ds region toward the 3′ terminus of the 5′ flap and 3-WJ (see below).

(D) Time course of KIAA1018 incubation with the indicated substrates (3:1 ratio protein to DNA). Whereas the 5′ flap was cut by KIAA1018 endonucleolytically, the 3-WJ lost its 5′ label due to KIAA1018 exonuclease activity. The 30-mer oligo of the 3-WJ is a good substrate for KIAA1018 exonuclease; its degradation gave rise to a 5′ flap substrate, which was then endonucleolytically cleaved by KIAA1018 (cf. panel A and Figure S4D). Labeling of the 3′ end of the 3-WJ showed also weak 5′→3′ degradation of the top strand.

(E) KIAA1018 exonuclease preferentially degrades dsDNA. Highest activity was observed on recessed, nicked, or gapped DNA substrates (10:1 ratio protein to DNA), whereas ss DNA and 5′ overhangs were poor substrates for KIAA1018.

(F) KIAA1018 incises 5′ flaps and then degrades the remaining strand in a 5′→3′ direction (20:1 ratio protein to DNA). In this experiment, the 5′ flap substrate was labeled either at the 5′ or the 3′ end of the 60-mer oligonucleotide f9 (Figure S4C) as indicated. The structures of the products are shown at the side of the autoradiograph.

(G) Comparison of substrate preference of KIAA1018, FEN1, and MUS81/EME1 (20:1 ratio protein to DNA). FEN1 and KIAA1018 prefer 5′ flaps, whereas MUS81/EME1 prefers 3′ flaps. All proteins were expressed in Sf9 cells.

(H) FLAG-KIAA1018 immunoprecipitated from stably transfected HEK293 cells showed the same specificity as the bacterially and Sf9-expressed recombinant KIAA1018 protein but made a more defined cut at the DNA junction.

All assays shown in this figure were carried out in magnesium. Samples were separated on denaturing 20% polyacrylamide gels for 1 hr at 40V/cm. The radioactive species were visualized by PhosphoImager (Typhoon 9400). M, oligonucleotide markers; WT, KIAA1018-WT; DA, KIAA1018 variant D960A. 3-WJ, 3-way junction. See Figure S4 for supplemental information.

with MLH1 did not affect the outcome of the nuclease assays (data not shown). We are currently analyzing the interactome of KIAA1018 in search for possible partners of this nuclease.

The substrate spectrum of KIAA1018 resembles that of FEN1, which displays preference for 5′ flaps (Harrington and Lieber, 1994). However, unlike KIAA1018, FEN1 made only a single cut, at the end of the ss flap (Figure 6G). In contrast, MUS81/EME1 failed to cleave the 5′ flap substrate but showed a clear preference for 3′ flaps, as reported (Kaliraman et al., 2001). We also included two D loop structures and a bubble in these experiments, as intermediates of recombination, but also as structures that arise transiently during DNA replication and transcription, processes blocked by cisplatin and MMC. Interestingly, the 5′ flaps of the D loop proved to be processed by the KIAA1018 endonuclease activity with similar efficiency to the 5′ flap, whereas only the exonuclease acted on the bubble and the 3′ flap substrates (Figure 6G, right panel).

The DA variant was used in parallel with the WT enzyme in the above assays. As processing of the tested substrates was almost undetectable (Figure 6, Figure S4), we conclude that

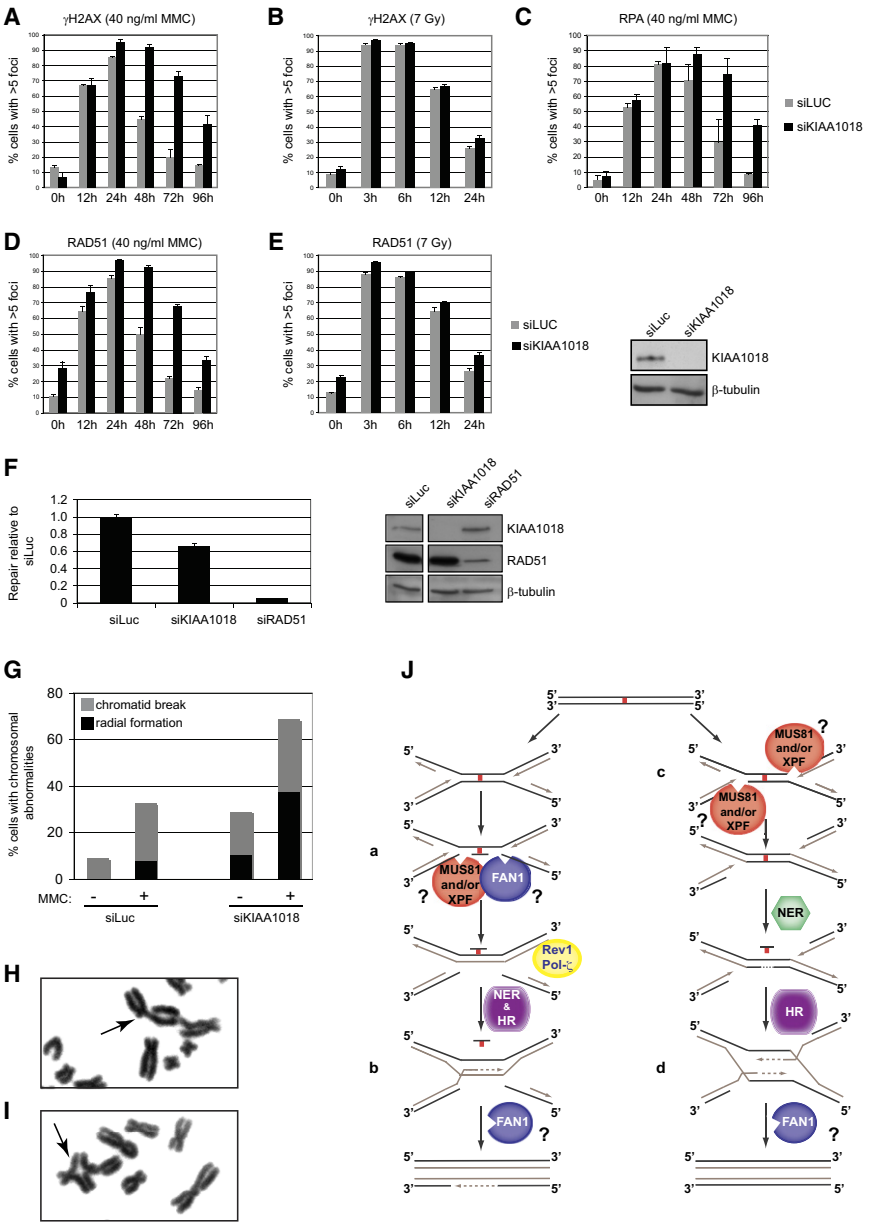


**Figure 7. KIAA1018 Is Involved in HR**

U2OS cells were treated with Luc or KIAA1018 siRNAs for 40 hr. Treatment with 40 ng/ml MMC (A, C, and D) or irradiation with 7 Gy (B and E) was followed by immunostaining with anti-γH2AX (A and B), anti-RPA (C), and anti-Rad51 (D and E) antibodies at the indicated time points after treatment. Graphs show % cells with more than five foci. In three independent experiments, 50 cells were counted per experiment. Each data point represents an average ± SD. Western blot showing efficiency of treatment with indicated siRNA for (A)–(E).

(F) Depletion of KIAA1018 results in a partial decrease of HR frequency compared to RAD51. HEK293 DR-GFP cells were transfected with siRNA against Luc (control), KIAA1018, and RAD51. Forty hours later, transfection with an I-SceI encoding plasmid or mock transfection were performed, followed by flow cytometric analysis 48 hr later. Approximately 1.1% of transfected cells pretreated with siRNA against Luc expressed GFP. Mock transfection did not result in GFP-positive cells. Graph represents the results of four independent experiments, each carried out in triplicate. Each data point represents an average ± SD.

(G–I) Depletion of KIAA1018 causes genomic instability. (G) Metaphase spreads of siLuc or siKIAA1018 transfected HEK293 cells treated or not with 25 ng/ml MMC for 20 hr were analyzed for chromatid breaks (H) and radial structures (I). Fifty spreads were analyzed per sample.

(J) Scheme of possible involvement of KIAA1018/FAN1 in the processing of ICLs. See text for details.

both the exo- and the endonuclease activities are inherent to the same active site of KIAA1018, rather than to a contaminant in the purified fractions.

## KIAA1018 Is Involved in the Repair of MMC-Induced Double-Strand Breaks

As shown in Figure 1A, processing of ICLs was suggested to involve endonucleolytic cleavage of the blocked replication forks by MUS81/EME1 and/or XPF/ERCC1. These one-ended double-strand breaks (DSBs) can be visualized directly by pulse-field gel electrophoresis (De Silva et al., 2000; Hanada et al., 2006), or indirectly as subnuclear foci of phosphorylated histone H2AX (γ-H2AX) (Niedernhofer et al., 2004; Rothfuss and Grompe, 2004). We wanted to test whether KIAA1018 depletion affected the formation and/or persistence of these DSBs. As shown in Figure 7A, 12 hr after MMC treatment, cells pretreated with KIAA1018 or control siRNAs contained ~6-fold more γ-H2AX foci than untreated controls. These foci reached a maximum at the 24 hr time point and then began to decline. This decline was substantially slower in cells depleted of KIAA1018, such that a considerable number of γ-H2AX foci were still present in the cells at the 96 hr time point. However, the KIAA1018-deficient cells do not appear to have a general defect in DSB repair, as treatment with IR induced similar numbers of γ-H2AX foci in cells pretreated with siRNA against KIAA1018 and Luc control (Figure 7B).

## KIAA1018 Deficiency Does Not Affect DSB Resection but Causes Delay in the Disappearance of RPA Foci

Repair of DSBs is accomplished by one of two principal pathways: nonhomologous end-joining (NHEJ) and HR (West, 2003). DSBs arising through the processing of ICLs are thought to be addressed predominantly by HR, whereby one strand of the broken duplex has to be resected in a 5′→3′ direction to generate long stretches of ssDNA. Given that KIAA1018 has

robust exonuclease activity, we wanted to find out whether it might be required for resection. The ssDNA generated during resection is coated first by RPA, and this process can be visualized in the form of RPA foci. As shown in Figure 7C, we observed a substantial increase of RPA foci in MMC-treated cells, but these appeared with similar kinetics in cells pretreated with siRNA against KIAA1018 and Luc. KIAA1018 thus does not appear to be required for DSB resection. However, after 96 hr, the RPA focus number returned nearly to untreated control levels, whereas the siKIAA1018 pretreated cells still displayed numerous foci.

### KIAA1018 Is Involved in HR

During HR, RAD51 displaces RPA on the ssDNA to generate filaments that invade homologous sequences on the sister chromatid (West, 2003). We analyzed the formation and disappearance of RAD51 foci in MMC-treated cells, pretreated with siRNA against KIAA1018 or Luc. We observed a 2- to 3-fold increase in RAD51 foci already in untreated cells, but this difference became less prominent in MMC-treated cells at the 12 and 24 hr time points, when the number of foci reached a maximum. However, at later time points, cells depleted of KIAA1018 contained more than twice as many RAD51 foci as the control (Figure 7D). This showed that KIAA1018 is not required for the early HR steps, but rather for their completion. As in the case of γ-H2AX foci (Figure 7B), no appreciable difference in the number of foci or the kinetics of their appearance and disappearance could be seen in the KIAA1018 and Luc siRNA pretreated cells upon irradiation (Figure 7E), which shows that the HR defect is limited to events induced by MMC.

In order to confirm this hypothesis, we deployed the reporter system described by Stark and colleagues (Bennardo et al., 2008), which monitors successful recombination events between two homologous DNA fragments integrated in the genome of HEK293 cells. Both these fragments encode defective *GFP* and one carries an engineered recognition site for the I-SceI endonuclease. Transfection of I-SceI cDNA into these cells leads to cleavage of one of the *GFP* copies. Cells in which the I-SceI-generated DSB is repaired by HR will express GFP. As shown in Figure 7F, HR was almost entirely abolished in cells pretreated with siRNA against RAD51, whereas siRNA against KIAA1018 reduced the efficiency of HR in this system by ~30%. This result confirms that KIAA1018 is involved in HR, but its role in the rescue of DSBs that did not arise as intermediates of ICL processing appears to be minor.

### KIAA1018 Deficiency Brings about Genomic Instability

Taken together, the evidence presented above implicates KIAA1018 specifically in the processing of damage induced by ICL-generating agents, which is one of the hallmarks of cells from FA patients. The latter cells also display considerable chromosomal instability (Akkari et al., 2000). Given the phenotypic similarity of FA- and KIAA1018-deficient cells, the dependence of KIAA1018 on FANCD2, and the above DSB repair defect, we examined metaphase chromosome spreads in HEK293 cells depleted either of KIAA1018 or of FANCJ by siRNA. As reported by others (Bridge et al., 2005), we detected a notable increase in chromosomal instability in FANCJ-depleted cells, where several chromosomal aberrations were frequently seen in single cells (data not shown). In KIAA1018-depleted cells, the chromosomal instability increase was much less pronounced. However, we noted an increase in aberrations already in untreated cells, and MMC treatment induced a 2-fold higher number of aberrations in KIAA1018-depleted cells as compared to the control siRNA pretreated cell population. Importantly, the increase in radial chromosome formation was 5-fold higher than in the control (Figures 7G–7I). Depletion of KIAA1018 thus brings about chromosomal instability reminiscent of that seen in cells of FA patients.

## DISCUSSION

As predicted by bioinformatic analysis (Kinch et al., 2005; Kosinski et al., 2005), KIAA1018 is indeed a nuclease with both endo- and exonuclease activities (Figure 5, Figure 6, Figure S3, and Figure S4). Due to its association with FANCD2, we propose to name it FAN1 (*F*ANCD2-*a*ssociated *n*uclease 1).

With its preference for 5′ flaps, FAN1 displays an opposite polarity to the two endonucleases implicated in ICL metabolism to date, MUS81/EME1 and XPF/ERCC1, both of which cleave preferentially 3′ flaps (Figure 6G and Ciccia et al., 2008). MUS81/EME1 is believed to initiate ICL repair by cleaving the leading-strand template of the blocked replication fork (Figure 1A, step c) and thus generate a one-ended DSB at the fork. The subsequent "unhooking" of the lesion (Figure 1A, step d) was proposed to involve XPF/ERCC1, but this is incongruent with its preference for 3′ flaps and is thus subject to some controversy (Ciccia et al., 2008). Recently, Walter and colleagues (Raschle et al., 2008) proposed an alternative mechanism of ICL repair, in which processing of the crosslink initiates only when replication forks traveling in opposite directions converge at the ICL (Figure 7J). In this scenario, FAN1 could work in concert with the 3′ flap-specific enzymes to unhook the ICL by cleaving the lagging-strand template (Figure 1A and Figure 7J, intermediate a) and thus help generate the substrate for the TLS polymerases Rev1 and pol-ζ (Raschle et al., 2008), which could later participate in the HR-mediated repair of the DSBs (Figure 7J, intermediate b). FAN1 might be involved also in the resolution of the HR intermediates. Although plausible, this mechanism has two caveats. First, the small size of the plasmid used made it likely that replication forks traveling in opposite directions would reach the ICL almost concurrently. This may not be the case in genomic DNA of higher eukaryotes, where replication origins are far apart. Moreover, ICLs activate a DNA-damage checkpoint that should prevent firing of late (or dormant) origins and thus reduce the chances of two forks colliding. The second caveat concerns the X-structure itself, inasmuch as MUS81/EME1 and/or XPF/ERCC1 could cleave both leading-strand templates of the X to generate two one-sided DSBs and a linear, but crosslinked, intermediate (Figure 7J, structure c). Both termini of this structure could be primer-extended to generate a substrate for excision repair. In this scenario, FAN1 would not be involved in the incision of the blocked fork, although it might participate in the repair of the two one-ended DSBs by HR (Figure 7J, intermediate d).

Data presented in Figure 7 support the involvement of FAN1 downstream from the replication fork cleavage. FAN1 deficiency

affected neither the formation of MMC-induced DSBs, as measured by the appearance of γ-H2AX foci (Figure 7A), nor their resection, as evidenced by RPA and RAD51 foci formation (Figures 7C and 7D respectively). However, it did affect DSB repair. Thus, even though the reduction in HR efficiency as measured by the GFP assay in HEK293 cells (Figure 7F) was only slight, the disappearance of RAD51 foci in vivo was substantially delayed (Figure 7D). Moreover, the chromosomal breaks and radials observed in FAN1-depleted MMC-treated cells strengthened the notion that FAN1 participates in HR and that, in its absence, MMC-induced lesions are processed erroneously, possibly by NHEJ, to give rise to the observed aberrations. Based on the above observations and coupled with evidence showing that repair of DSBs induced by IR was unaffected by FAN1 status, and that FAN1 depletion did not alter the sensitivity of cells to IR and camptothecin (Figures 2B and 2D), as well as methyl methane sulfonate (MMS) and HU (data not shown), we propose that FAN1 is required for the processing of recombination intermediates that arise predominantly during the metabolism of damage induced by ICL-generating agents. The elucidation of the molecular role of FAN1 will have to await the results of studies deploying a defined system, such as that described by the Walter laboratory (Raschle et al., 2008).

Our findings that the recruitment of FAN1 to MMC-induced foci is dependent on FANCD2 ubiquitylation, and that the two proteins appear to physically interact, represent strong evidence in support of an involvement of this nuclease in the FA-dependent pathway of ICL repair. It remains to be seen whether *FAN1* is a *FA* gene. To date, FA patients fall into 13 complementation groups that are linked to mutations in the *FANCA, B, C, D1, D2, E, F, G, I, J, L, M*, and *N* genes. However, several patients are yet to be assigned, and we are in the process of screening the DNA of these individuals for germline mutations in *FAN1.*

## EXPERIMENTAL PROCEDURES

cDNA, vectors, antibodies, cell lines, protein purifications, and standard procedures are described in Extended Experimental Procedures.

### Immunofluorescence Staining and Laser-Induced Damage

U2OS cells cultured on coverslips were mock-treated or treated with 120 ng/ml MMC and fixed 16 or 20 hr later with 3% formaldehyde/PBS for 15 min at 4°C. Membranes were permeabilized with 0.2% Triton X-100 in PBS for 5 min at 4°C. Samples were blocked with 3% nonfat milk/PBS and incubated with primary antibodies overnight at 4°C and with secondary antibodies for 1 hr at 37°C. DNA was stained with DAPI. Slides were analyzed using an Olympus IX81 or a Zeiss LSM710 confocal microscope (sequential scanning mode).

Ten micromoles of BrdU was added to the cells 24 hr prior to laser microirradiation. Laser stripes were induced with a laser beam (λ = 355 nm) at 50% power using the 40× objective. Cells were fixed 2 hr later.

### siRNA Treatments and Cell Survival Assays

HEK293 cells were transfected with siRNAs in 6-well plates at 60% confluency using calcium phosphate. For survival assays, cells were seeded 24 hr after transfection in triplicates in 6-well plates at a density of 400 cells per well. Sixteen hours after seeding, the cells were treated with indicated concentrations of MMC, cisplatin, camptothecin, UV, or IR. Medium was replaced 24 hr (MMC and cisplatin), 1 hr (camptothecin), or directly (UV, IR) after treatment. After 8 days, the cells were fixed and stained with 0.5% crystal violet in 20% ethanol and colonies containing more than 50 cells were counted.

### Specific Nuclease Assays

#### *Endonuclease Assays*

One nanomole of labeled substrate was incubated with 10 nmole (or as indicated) of KIAA1018 WT or its variants in 25 mM HEPES-KOH (pH 7.4), 25 mM KCl, 1 mM $MnCl_2$ or $MgCl_2$ as indicated, and 0.05 mg/ml BSA for 30 min at 37°C. The reaction was terminated with 0.1% SDS, 14 mM EDTA, and 0.1 mg/ml Proteinase K and incubation at 55°C for 15 min. Loading buffer was added and the samples were separated on a 20% denaturing polyacrylamide gel for 1 hr at 40 V/cm. The gels were dried and the bands were visualized on a PhosphoImager.

#### *Exonuclease Assays*

These were carried out as above, using the substrates indicated at the bottom of the panels in Figure 6E and Figure S4G.

### Endonuclease Assays with FLAG-KIAA1018 Immunoprecipitate from HEK293 Cells

Stably transfected HEK293 cells expressing 3×FLAG-KIAA1018 were grown on 15 cm dishes with G418 to 80% confluency. The cells were pelleted by centrifugation, washed in PBS, and snap-frozen. The pellets were lysed (50 mM Tris-HCl pH 7.4, 150 mM NaCl, 1% Triton, protease inhibitors) and incubated on ice for 20 min. The lysate was centrifuged and incubated with mouse anti-FLAG M2-Agarose (Sigma) for 2 hr at 4°C on a rotating wheel (300 rpm). Subsequently, the beads were washed twice for 15 min with 500 μl wash buffer (50 mM Tris-HCl pH 7.4, 150 mM NaCl, and 1 μg/ml BSA), then twice for 15 min with 500 μl with elution buffer (62.5 mM HEPES-KOH pH 7.4, 62.5 mM KCl, 5% glycerol, and 1 mM DTT). FLAG-KIAA1018 was eluted with FLAG-peptides (150 ng/μl, Sigma) in a total volume of 70 μl for 30 min at 4°C on a shaker (600 rpm).

### Homologous Recombination Assay

This was carried out essentially as described (Bennardo et al., 2008). Details can be found in the Extended Experimental Procedures.

## SUPPLEMENTAL INFORMATION

Supplemental Information includes Extended Experimental Procedures and four figures and can be found with this article online at doi:10.1016/j.cell.2010.06.022.

## ACKNOWLEDGMENTS

We express our gratitude to John Rouse for the KIAA1018 antibody and for sharing unpublished information, to Milica Enoiu for discussions and for critical reading of the manuscript, Stephanie Felscher for help with evaluation of chromosomal instability, Myriam Marti for help with western blot analyses, Ian Hickson for MUS81/EME1, Ulrich Hübscher for FEN1, Pavel Janscak and Rajakrishnan Kanagaraj for the oligonucleotides, Jordi Surralles for the FANCD2-deficient and WT- or K561R- complemented PD20 cells, Petr Cejka for the Sf9 expression system, and Stefano Ferrari for MG132. We also acknowledge collaborations with Johan de Winter and Hans Joenje and with the group of Shunichi Takeda. The *C01G5.8(tm423)* deletion allele was kindly provided by Dr. Shohei Mitani (Japanese National Bioresource Project). This work was supported by Swiss National Science Foundation grants nr. 3100A0-118158 (J.J.) and 3100A0-128675 (M.H.). The generous support of the Bonizzi-Theler (J.J.) and Ernst Hadorn (M.H.) Foundations is also gratefully acknowledged.

Received: March 3, 2010
Revised: May 29, 2010
Accepted: June 15, 2010
Published: July 8, 2010

## REFERENCES

Akkari, Y.M., Bateman, R.L., Reifsteck, C.A., Olson, S.B., and Grompe, M. (2000). DNA replication is required To elicit cellular responses to psoralen-induced DNA interstrand cross-links. Mol. Cell. Biol. *20*, 8283–8289.

Bennardo, N., Cheng, A., Huang, N., and Stark, J.M. (2008). Alternative-NHEJ is a mechanistically distinct pathway of mammalian chromosome break repair. PLoS Genet. *4*, e1000110.

Bridge, W.L., Vandenberg, C.J., Franklin, R.J., and Hiom, K. (2005). The BRIP1 helicase functions independently of BRCA1 in the Fanconi anemia pathway for DNA crosslink repair. Nat. Genet. *37*, 953–957.

Cannavo, E., Gerrits, B., Marra, G., Schlapbach, R., and Jiricny, J. (2007). Characterization of the interactome of the human MutL homologues MLH1, PMS1, and PMS2. J. Biol. Chem. *282*, 2976–2986.

Ciccia, A., McDonald, N., and West, S.C. (2008). Structural and functional relationships of the XPF/MUS81 family of proteins. Annu. Rev. Biochem. *77*, 259–287.

Dantuma, N.P., Groothuis, T.A., Salomons, F.A., and Neefjes, J. (2006). A dynamic ubiquitin equilibrium couples proteasomal activity to chromatin remodeling. J. Cell Biol. *173*, 19–26.

De Silva, I.U., McHugh, P.J., Clingen, P.H., and Hartley, J.A. (2000). Defining the roles of nucleotide excision repair and recombination in the repair of DNA interstrand cross-links in mammalian cells. Mol. Cell. Biol. *20*, 7980–7990.

Ermolova, N.V., Ann Cushman, M., Taybi, T., Condon, S.A., Cushman, J.C., and Chollet, R. (2003). Expression, purification, and initial characterization of a recombinant form of plant PEP-carboxylase kinase from CAM-induced Mesembryanthemum crystallinum with enhanced solubility in Escherichia coli. Protein Expr. Purif. *29*, 123–131.

Garcia-Higuera, I., Taniguchi, T., Ganesan, S., Meyn, M.S., Timmers, C., Hejna, J., Grompe, M., and D'Andrea, A.D. (2001). Interaction of the Fanconi anemia proteins and BRCA1 in a common pathway. Mol. Cell *7*, 249–262.

Gari, K., Decaillet, C., Stasiak, A.Z., Stasiak, A., and Constantinou, A. (2008). The Fanconi anemia protein FANCM can promote branch migration of Holliday junctions and replication forks. Mol. Cell *29*, 141–148.

Hanada, K., Budzowska, M., Modesti, M., Maas, A., Wyman, C., Essers, J., and Kanaar, R. (2006). The structure-specific endonuclease Mus81-Eme1 promotes conversion of interstrand DNA crosslinks into double-strands breaks. EMBO J. *25*, 4921–4932.

Harrington, J.J., and Lieber, M.R. (1994). The characterization of a mammalian DNA structure-specific endonuclease. EMBO J. *13*, 1235–1246.

Hofmann, K. (2009). Ubiquitin-binding domains and their role in the DNA damage response. DNA Repair (Amst.) *8*, 544–556.

Kadyrov, F.A., Holmes, S.F., Arana, M.E., Lukianova, O.A., O'Donnell, M., Kunkel, T.A., and Modrich, P. (2007). Saccharomyces cerevisiae MutLalpha is a mismatch repair endonuclease. J. Biol. Chem. *282*, 37181–37190.

Kaliraman, V., Mullen, J.R., Fricke, W.M., Bastin-Shanower, S.A., and Brill, S.J. (2001). Functional overlap between Sgs1-Top3 and the Mms4-Mus81 endonuclease. Genes Dev. *15*, 2730–2740.

Kinch, L.N., Ginalski, K., Rychlewski, L., and Grishin, N.V. (2005). Identification of novel restriction endonuclease-like fold families among hypothetical proteins. Nucleic Acids Res. *33*, 3598–3605.

Kosinski, J., Feder, M., and Bujnicki, J.M. (2005). The PD-(D/E)XK superfamily revisited: identification of new members among proteins involved in DNA metabolism and functional predictions for domains of (hitherto) unknown function. BMC Bioinformatics *6*, 172.

Meetei, A.R., Sechi, S., Wallisch, M., Yang, D., Young, M.K., Joenje, H., Hoatlin, M.E., and Wang, W. (2003). A multiprotein nuclear complex connects Fanconi anemia and Bloom syndrome. Mol. Cell. Biol. *23*, 3417–3426.

Moldovan, G.L., and D'Andrea, A.D. (2009). How the fanconi anemia pathway guards the genome. Annu. Rev. Genet. *43*, 223–249.

Niedernhofer, L.J., Odijk, H., Budzowska, M., van Drunen, E., Maas, A., Theil, A.F., de Wit, J., Jaspers, N.G., Beverloo, H.B., Hoeijmakers, J.H., et al. (2004). The structure-specific endonuclease Ercc1-Xpf is required to resolve DNA interstrand cross-link-induced double-strand breaks. Mol. Cell. Biol. *24*, 5776–5787.

Peng, M., Litman, R., Xie, J., Sharma, S., Brosh, R.M., Jr., and Cantor, S.B. (2007). The FANCJ/MutLalpha interaction is required for correction of the cross-link response in FA-J cells. EMBO J. *26*, 3238–3249.

Pichierri, P., and Rosselli, F. (2004). The DNA crosslink-induced S-phase checkpoint depends on ATR-CHK1 and ATR-NBS1-FANCD2 pathways. EMBO J. *23*, 1178–1187.

Raschle, M., Knipscheer, P., Enoiu, M., Angelov, T., Sun, J., Griffith, J.D., Ellenberger, T.E., Scharer, O.D., and Walter, J.C. (2008). Mechanism of replication-coupled DNA interstrand crosslink repair. Cell *134*, 969–980.

Rothfuss, A., and Grompe, M. (2004). Repair kinetics of genomic interstrand DNA cross-links: evidence for DNA double-strand break-dependent activation of the Fanconi anemia/BRCA pathway. Mol. Cell. Biol. *24*, 123–134.

Smogorzewska, A., Matsuoka, S., Vinciguerra, P., McDonald, E.R., 3rd, Hurov, K.E., Luo, J., Ballif, B.A., Gygi, S.P., Hofmann, K., D'Andrea, A.D., et al. (2007). Identification of the FANCI protein, a monoubiquitinated FANCD2 paralog required for DNA repair. Cell *129*, 289–301.

Thompson, L.H., and Hinz, J.M. (2009). Cellular and molecular consequences of defective Fanconi anemia proteins in replication-coupled DNA repair: mechanistic insights. Mutat. Res. *668*, 54–72.

Wang, W. (2007). Emergence of a DNA-damage response network consisting of Fanconi anaemia and BRCA proteins. Nat. Rev. Genet. *8*, 735–748.

West, S.C. (2003). Molecular views of recombination proteins and their control. Nat. Rev. Mol. Cell Biol. *4*, 435–445.

Zhang, N., Lu, X., Zhang, X., Peterson, C.A., and Legerski, R.J. (2002). hMutSbeta is required for the recognition and uncoupling of psoralen interstrand cross-links in vitro. Mol. Cell. Biol. *22*, 2388–2397.